

Structure of transition-metal–oxygen–vacancy pair centers

E. Siegel* and K. A. Müller

IBM Zurich Research Laboratory, 8803 Rüschlikon, Switzerland

(Received 8 September 1977)

The microscopic structure of the $\text{Fe}^{3+}\text{-}V_{\text{O}}$ and $\text{Mn}^{2+}\text{-}V_{\text{O}}$ pair centers has been considered using the Newman superposition model. This model yields the EPR parameter b_2^0 as a function of transition-metal–oxygen distance d and position. It is found, for the oxide perovskites, that the transition-metal ion moves by a distance $\Delta = 0.1 d = 0.2 \text{ \AA}$ towards the vacancy V_{O} . The four lateral oxygens move against the metal ion by 4% or 0.08 \AA . This is in agreement with the reduction of the metal ionic radius due to the five-fold coordination. The intrinsic two-center parameter \bar{b}_2 needed in the Newman model is based on the uniaxial strain data of MgO and SrTiO_3 , as well as on the measured spin-Hamiltonian parameter b_2^0 in the tetragonal phase of SrTiO_3 . The \bar{b}_2 parameters obtained also provide information on other centers reported in oxide and fluoride compounds.

I. INTRODUCTION

More than a decade ago, in the cubic perovskite-type crystal SrTiO_3 , a new kind of defect was discovered by electron paramagnetic resonance. It consisted of a trivalent iron ion Fe^{3+} exposed to a large axial crystal field. It was postulated to consist of an Fe^{3+} ion on an octahedral Ti^{4+} site next to an oxygen vacancy.¹ Such a defect is possible in perovskite-type ABO_3 crystals in which the B ion has a high nominal valency, i.e., Ti^{4+} or Nb^{5+} for charge-compensating reasons. It is much less likely to occur in cubic NaCl-type oxides like MgO, where the Mg ion is twofold positively charged. In MgO, Cr^{3+} centers with Mg vacancies (V_{Mg}) on nearest-neighbor lattice sites have been identified with defect axes along $\langle 110 \rangle$ directions² and on next-nearest-neighbor lattice sites along $\langle 100 \rangle$ directions.^{3,4}

Since the discovery of the $\text{Fe}^{3+}\text{-}V_{\text{O}}$ center in SrTiO_3 , many such pair centers have been observed by EPR with the general formula $M\text{-}V_{\text{O}}$ in perovskite-type crystals, where M stands for transition-metal ions of valency 2 or 3.⁵ Recently, one was found with valency 4, i.e., the $\text{Fe}^{4+}\text{-}V_{\text{O}}$ center.⁶ The pair center most thoroughly characterized by EPR is still the $\text{Fe}^{3+}\text{-}V_{\text{O}}$.⁵ In this paper, we try to gain an understanding of the local environment of this center based on the axial EPR parameter b_2^0 measured and the reduced octahedral rotation angle $\bar{\varphi}$ below the cubic-to-tetragonal phase transition in SrTiO_3 .⁵ This was possible due to very recent advances in the field—first, the center isoelectric to $\text{Fe}^{3+}\text{-}V_{\text{O}}$, the $\text{Mn}^{2+}\text{-}V_{\text{O}}$, was observed by EPR and analyzed,⁷ and second, the superposition model for EPR spin-Hamiltonian parameters for rare-earth compounds of Newman⁸ was extended by him, Urban,^{9,10} and Siegel¹¹ to transition-metal ions.

The essence of the Newman model is reviewed in Sec. II. This allows the distortion of the five oxygens around the Fe^{3+} and Mn^{2+} isoelectronic center to be analyzed, if the parameter of the linear superposition model is known. The latter is obtained from EPR and crystallographic data of Fe^{3+} or Mn^{2+} ions with octahedral oxygen and fluorine coordination without a nearby vacancy (see Sec. III). In Sec. IV, we then use these data to estimate the local distortion around the $\text{Fe}^{3+}\text{-}V_{\text{O}}$ and $\text{Mn}^{2+}\text{-}V_{\text{O}}$ centers, and show that the Fe^{3+} and Mn^{2+} ions move about 0.2 \AA towards the vacancy.

With the linear superposition parameters obtained in Sec. III, it is also possible to verify the assignment of models for axial EPR centers reported in oxide and fluorine perovskite compounds, as well as for SrO and MgO. The analysis done in Sec. V on two tetragonal, strongly axial centers in $\text{MgO}:\text{Fe}^{3+}$,¹² and $\text{SrO}:\text{Mn}^{2+}$,¹³ points to probable $\text{Fe}^{3+}\text{-}V_{\text{O}}$, $\text{Mn}^{2+}\text{-}V_{\text{O}}$ pair centers, respectively. This indicates more frequent occurrence of $M\text{-}V_{\text{O}}$ pair centers than expected previously. The nature of the axial Fe^{3+} centers with five fluorines around the Fe^{3+} ion in KMgF_3 ,¹⁴ KZnF_3 ,¹⁵ and RbCdF_3 (Ref. 16) is undertaken. It is shown that the sign of b_2^0 determines whether the centers are $\text{Fe}^{3+}\text{-}V_{\text{F}}$ pair centers or if they consist of distorted FeOF_5 octahedra with one O^{2-} ion present. Finally, a reassignment of the cubic Mn^{2+} spectrum in BaTiO_3 as being due to octahedrally coordinated Mn^{2+} (see Ref. 17) is carried out in Appendix A. The tetragonal Mn^{2+} center in KTaO_3 found by Hannon¹⁸ is discussed in Appendix B.

II. NEWMAN LINEAR-SUPERPOSITION MODEL

This model assumes that the spin-Hamiltonian parameters b_n^m result from a linear superposition

of single ligand contributions of the form

$$b_n^m = \sum_i \bar{b}_n(R_i) K_n^m(\theta_i, \varphi_i). \quad (1)$$

The $K_n^m(\theta_i, \varphi_i)$ are spherical harmonic functions of rank n of the polar angles. For example, $K_2^0 = \frac{1}{2}(3 \cos^2 \theta - 1)$ or $K_2^2 = \frac{3}{2} \sin^2 \theta \cos 2\varphi$. The $\bar{b}_n(R)$ are functions of the radial metal-ligand distance R which are called the intrinsic parameters. They differ for various paramagnetic ions, i.e., Fe^{3+} or Mn^{2+} , as well as for oxygen or fluorine ligands.^{8,10} So far, it has been assumed that the functional form of $\bar{b}_2(R)$ obeys a single potential law term

$$\bar{b}_2(R_i) = \bar{b}_2(R_0)(R_0/R_i)^{t_2}, \quad (2)$$

where the power-law exponent is of the order 10. In certain cases, however, a sum of two exponentials had to be taken.¹⁰ R_0 is the reference distance, and R_i the one to the ligand ion i . The b_n^m are the spin-Hamiltonian parameters for which the symbols D , E , a , and F are often used. They are related to one another by

$$b_2^0 = D, \quad b_2^2 = 3E, \quad b_4^4 = \frac{5}{2}a, \quad b_4^0 = \frac{1}{2}a + \frac{1}{3}F.$$

The summation in Eq. (1) goes over the nearest-neighbor ligands of the paramagnetic ion. The essential idea behind this model¹⁹ is the following: the measured spin-Hamiltonian parameters are, to a large percentage, given by covalent effects, i.e., overlap and exchange with the nearest neighbors. The normal crystal-field contributions, especially for the lower $n=2$ rank constants b_2^m , are inherently of longer range. Thus the employment of the crystal field for calculating EPR spin-Hamiltonian parameters b_2^m is bound to fail.

For rare-earth impurities, the assumption of linear superposition as in Eq. (1) has been proven successful. For the even more covalently bound transition-metal ions, consistent results were first accumulated by Newman and Siegel,¹¹ and are corroborated by the results in Sec. III. Nonlinear three-body interactions appear to be negligible so far.

The Newman model correlates spin-Hamiltonian parameters measurable from EPR experiments with positions of ligands available from crystallographic data. The $\bar{b}_n(R)$ are parameters which one has to determine from centers whose natures are known and for which EPR and crystallographic data are available. With the known function $\bar{b}_n(R)$, two applications are possible: (i) An analysis of local arrangements, if the EPR parameters are known and if the symmetry is sufficiently high. (ii) Predictions of the sign and magnitude of spin-Hamiltonian parameters can be made if, for

a local configuration, the crystallographic data are available. Thus the assignment of centers can be verified or discarded.

The aim of this paper is primarily laid out in application (i) for the oxygen vacancy centers, while (ii) may be used to verify certain models. To do this, we need the parameters $\bar{b}_n(R)$. In Sec. III, we therefore determine these quantities from single paramagnetic impurity centers of some perovskite and other compounds, and compare them with the results obtained earlier in Ref. 11. Since the pair-vacancy centers to which we refer are axial, and the spin-Hamiltonian parameter $D = b_2^0$ is the largest of all, we restrict ourselves in the following consideration to the $n=2$ parameters. As a model equation we use Eq. (3), which results from Eqs. (1) and (2):

$$b_2^m = \bar{b}_2(R_0) \left[\sum_i \left(\frac{R_0}{R_i} \right)^{t_2} K_2^m(\theta_i, \varphi_i) \right]. \quad (3)$$

A very important relation can be deduced from it that gives a rough and quick estimate whether two different paramagnetic ions such as Fe^{3+} and Mn^{2+} are on the same site in a compound. To get the relation we assume that both the local surrounding and the power-law exponents of both paramagnetic ions I and II are identical. Then we get

$$b_2^{0(\text{I})}/b_2^{0(\text{II})} = \bar{b}_2^{(\text{I})}/\bar{b}_2^{(\text{II})}, \quad (4)$$

where $\bar{b}_2^{(\text{I})}$ and $\bar{b}_2^{(\text{II})}$ are the intrinsic parameters for the two paramagnetic ions, taken at the same distance R_0 . Because the paramagnetic ions—for example, Fe^{3+} and Mn^{2+} —have different sizes and charges, the surrounding as well as t_2 will be somewhat different. Therefore, this relation is only approximately fulfilled but is quite useful.

III. DETERMINATION OF \bar{b}_2

A. \bar{b}_2 for Fe^{3+} and Mn^{2+} in oxide compounds

Essential for the model calculations of Secs. IV and V is the knowledge of parameters $\bar{b}_2(R_0)$ and t_2 . From uniaxial strain data of cubic crystals, it is possible to determine these two parameters independently. The result of the analysis on MgO and CaO of Newman and Siegel¹¹ is shown in Table I, which also includes the values for Fe^{3+} in SrTiO_3 . In the case of SrTiO_3 the \bar{b}_2 values were evaluated in two ways. (i) The measured uniaxial strain parameter $G_{11} = 7.26(20) \text{ cm}^{-1}$ per unit strain of Waldkirch and Müller²⁰ in the cubic phase allows the determination of the product of \bar{b}_2 and t_2 using $G_{11} = -\frac{4}{3}t_2\bar{b}_2$.¹¹ One obtains $\bar{b}_2 t_2 = -5.45(15) \text{ cm}^{-1}$. (ii) On the other hand, \bar{b}_2 can be obtained combining the crystallographic data of Refs. 21–

TABLE I. Intrinsic parameters \bar{b}_2 for Fe^{3+} and Mn^{2+} in some oxide perovskite compounds.

		Model parameters for Fe^{3+}		
		R_0 (Å)	\bar{b}_2 (cm^{-1})	t_2
MgO	strain data	2.101	-0.412(25)	8(1)
CaO	strain data	2.398	-0.225(20)	5(1)
SrTiO ₃	tetr. phase	1.952	-0.57(38)	8(1) assumed
SrTiO ₃	strain data	1.952	-0.68(10)	8(1) assumed
		Model parameter for Mn^{2+}		
		R_0 (Å)	\bar{b}_2 (cm^{-1})	t_2
MgO	strain data	2.101	-0.157(5)	7(1)
CaO	strain data	2.398	-0.050(10)	7(1)

23 with the EPR data of Ref. 24 of the tetragonal phase. Using model Eq. (3) for the tetragonal distorted octahedra with distance $\frac{1}{2}c$ and $\frac{1}{2}a'$ to the nearest neighbors of Fe^{3+} , one gets

$$b_2^0 = \bar{b}_2(R_0 = \frac{1}{2}c) \times 2[1 - (c/a')^2]. \quad (5)$$

Because the ratio $c/a' = 1 + 0.8(4) \times 10^{-4}$ (Ref. 23) is near one, Eq. (5) can be expanded, resulting in

$$b_2^0 = -\bar{b}_2(R_0)t_2 \times 2(c/a' - 1). \quad (6)$$

This shows that only the product of \bar{b}_2 and t_2 is accessible. With $b_2^0 = 7.3(3) \times 10^{-4} \text{ cm}^{-1}$ of Ref. 24 and the value of c/a' , one obtains

$$\bar{b}_2(R_0)t_2 = -4.6 \pm 2.5 \text{ cm}^{-1}.$$

The R_0 value of SrTiO₃ is close to that of MgO; thus we assume that the power-law exponent t_2 is the same as in MgO. With this assumption we get the values for Fe^{3+} in SrTiO₃ in Table I. Both \bar{b}_2 values of SrTiO₃ are consistent within the error limits; they are also in the range of \bar{b}_2 extrapolated from MgO for R_0 of SrTiO₃ [$\bar{b}_2(1.952 \text{ Å}) = -0.74(11) \text{ cm}^{-1}$]. From this, we conclude that the potential law of Eq. (2), with the data of MgO of Table I, is a good basis for model calculations in an R_0 distance range of 1.9–2.1 Å. The values of Mn^{2+} in oxides of Ref. 11 are also included in Table I. These data, mainly based on uniaxial strain data, build the basis for our model calculations of Secs. IV and V.

Since we want to interpret the $M-V_0$ centers in perovskites, it would have been suggestive to determine \bar{b}_2 and t_2 from other distorted oxide perovskites, for which intrinsic crystallographic and Fe^{3+} or Mn^{2+} EPR data are known. Candidates for this are ferroelectric tetragonal^{17,25,26} and orthorhombic BaTiO₃,^{26,27} orthorhombic KNbO₃,^{28,29} and tetragonal PbTiO₃.^{30–32} However due to the large distortions and the inner dipolar electric fields, there are doubts about the exact position of the Fe^{3+} or Mn^{2+} ion because of the different

charge. Since this exact position is the essential point for determining the intrinsic parameters, these compounds had to be omitted.

Employing for these compounds the same \bar{b}_2 and t_2 parameters for Fe^{3+} and Mn^{2+} as in Table I, and allowing for an additional shift Δ of the center of the ions along the polar [100], [110], or [111] axes in the tetragonal orthorhombic and rhombohedral phases, respectively, the various observed b_2^0 , b_2^2 parameters could very recently be explained self-consistently. The shift Δ thus derived always has a negative sign such that the Fe^{3+} and Mn^{2+} ions are close to the center of inversion of the octahedron. This means that the Fe^{3+} and Mn^{2+} ions participate *less* in the ferroelectric phase transition than do the bulk Ti^{4+} or Nb^{5+} ions. This is consistent with the earlier observation of Arend,³³ who found that Fe^{3+} doping always reduces the T_c of BaTiO₃. The detailed results of our calculations will be published separately. Note that in SrTiO₃ or MgO, such a shift Δ cannot exist at the Ti^{4+} or Mg^{2+} sites, since both compounds have the symmetry O_h at the cation site. This further adds to the consistency of the use of \bar{b}_2 and t_2 as derived from these two compounds.

In passing, we note that it is stated in Newman and Siegel's paper¹¹ that \bar{b}_2 is positive for the scheelite compounds CaWO₄ and SrWO₄, but in both substances the value of \bar{b}_2 is negative, as can be seen from Table II. In this calculation, we assumed that Mn^{2+} is located on the Ca and Sr sites, respectively, as discussed in Refs. 35 and 36. Apart from this we can assign this Mn^{2+} center from the hyperfine-structure constant $\bar{A} = \frac{1}{3}(A + 2B)$, which in CaWO₄ is $-89.3(1) \times 10^{-4} \text{ cm}^{-1}$,³⁵ and in SrWO₄ is $-89.7(1) \times 10^{-4} \text{ cm}^{-1}$,³⁶ respectively. Using the covalency parameter of Gordy and Thomas³⁷ and Eq. (2) of Šimánek and Müller,³⁸ one obtains for the Mn-O bond $C \approx 0.5$. In the scheelite compounds, there are two cation sites: the W site, which is four-fold, and the Ca site, which is eightfold coordinated. Using the A vs c/n curve of Ref. 38, we get for $n=4$ ligands $A \approx -79 \times 10^{-4} \text{ cm}^{-1}$ and for $n=8$, $A \approx -92 \times 10^{-4} \text{ cm}^{-1}$. Therefore, the Mn^{2+} ion occupies the Ca place. Using the $\bar{b}_2(R)$ function for MgO and CaO (Table I), we obtain for the distances given in Table II somewhat larger absolute values for \bar{b}_2 than those calculated from the EPR data.

B. \bar{b}_2 for Fe^{3+} in fluoride perovskite compounds

There are only a few compounds with fluorine ligands where the Fe^{3+} paramagnetic-ion parameters are known. From the tetragonal phase of TlCdF₃,³⁹ RbCdF₃,⁴⁰ and RbCaF₃,⁴¹ it is possible

TABLE II. Intrinsic parameters \bar{b}_2 for Mn^{2+} in the scheelite compounds CaWO_4 and SrWO_4 . Model equation: $b_2^0 = \bar{b}_2(R_0) [4K_2^0(\theta_1)(1 - t_2\Delta/R_0) + 4K_2^0(\theta_2)]$.

	θ_1	θ_2	$4K_2^0(\theta_1)$	$4K_2^0(\theta_2)$	Δ/R_0	R_0 (Å)	Ref. cryst. data
CaWO_4	66.73 ⁰	139.88 ⁰	-1.0635	+1.5086	0.017	2.438	34
SrWO_4	68.00 ⁰	141.20 ⁰	-1.1580	+1.6442	0.012	2.579	34
	b_2^0 (10^{-4} cm ⁻¹)	Temp. T (K)	Ref. EPR data		$\bar{b}_2(R_0)$ (10^{-4} cm ⁻¹) assuming $t_2=7$		
CaWO_4	-137.6(3)	77	35		-241.3		
SrWO_4	-107.7(3)	4.2	36		-184.5		
	$\bar{b}_2(R_0)$ (10^{-4} cm ⁻¹) extr. MgO		$\bar{b}_2(R_0)$ (10^{-4} cm ⁻¹) extr. CaO				
CaWO_4	-560(100)		-440(100)				
SrWO_4	-370(90)		-300(80)				

to determine the product of \bar{b}_2 and t_2 with the use of the same model equation [Eq. (6)] as in tetragonal SrTiO_3 . To evaluate c/a' we used the relation of Alefeld,²³

$$c(T)/a'(T) = [1 + (\Delta c - \Delta a)/c_0] \cos\varphi.$$

In this equation, c_0 is the lattice constant at T_c . The deviations from c_0 at the temperature T along the a and c axes are Δa and Δc , respectively. R_0 was chosen as $R_0 = \frac{1}{2}c$ at the temperature T . All of these values were obtained from $a(T)$ and $c(T)$ curves given in Table III, column 6. In the equation, φ is the tilting angle of the CdF_6 and CaF_6 octahedra around the c axis. This angle was obtained in the case of RbCdF_3 from EPR experiments. For the other two compounds, we employed the relation $c/a - 1 = \frac{3}{2}\varphi^2$ derived and verified by Rousseau *et al.*⁴⁰ to determine φ . The b_2^0 values were also obtained from $b_2^0(T)$ curves cited in Table III, column 7. With these EPR and crystallographic data, $\bar{b}_2(R_0)t_2$ in Table III was obtained. If we assume that the power-law exponents t_2 for fluorine and oxygen ligands are the same and equal to $t_2 = 8$, we get the last column of Table III.

The K^+ vacancy center in $\text{KZnF}_3:\text{Fe}^{3+}$ was analyzed by electron-nuclear double resonance (ENDOR).⁴⁴ From these measurements, it is possible to determine \bar{b}_2 . The ENDOR data showed that the angular distortions at 4.3 K are $\varphi_1 = 57.5^\circ(3)$ and $\varphi_2 = 126.4^\circ(3)$. Together with the value of $b_2^0 = +107.9(3) \times 10^{-4}$ cm⁻¹ at 77 K and assuming that the distances to all fluorines are equal ($R_0 = 2.027$ Å), we get $\bar{b}_2(R_0) = -0.089(32)$ cm⁻¹. In this result no implicit t_2 dependence is involved. The error in \bar{b}_2 is a result of the error in the angles of 0.3° . Comparing this value

with those of Table III (last column), we see that they are the same within the error limits. We conclude therefore that t_2 for the fluorine compounds is in the range of $t_2 \approx 8$.

From these calculations, for the Fe^{3+} as paramagnetic ion with fluorine as ligand, we get the result that the intrinsic parameter \bar{b}_2^F is negative, its absolute magnitude being two to three times smaller than that of the oxygen intrinsic parameter \bar{b}_2^O , and t_2 is in the range of eight as for the oxygen ligands.

IV. LOCAL ENVIRONMENT OF $M-V_O$ PAIR CENTERS IN OXIDE PEROVSKITE COMPOUNDS

With the \bar{b}_2 values of Sec. III, it is possible to gain information about the distortion of the vacancy pair centers. These centers consist of a paramagnetic impurity ion placed on the B site of the ABO_3 structure surrounded by five oxygens. From the experimental point of view, these centers are characterized by the very large value of b_2^0 compared with centers without next-neighbor vacancies and by the positive sign of this parameter. To compare the different compounds, we use the quantity $b_2^0/\bar{b}_2(d)$. Here b_2^0 is the measured spin-Hamiltonian parameter and $\bar{b}_2(d)$ is the intrinsic parameter for Fe^{3+} and Mn^{2+} , respectively, and oxygen ligands at the undistorted distance d . This is the position at which the paramagnetic ion would be without vacancy. The use of $b_2^0/\bar{b}_2(d)$ comes from Eq. (3), which correlates b_2^0 with $\bar{b}_2(d)$ and the ligand surroundings. In Table IV, the pertinent parameters for the $\text{Fe}^{3+}-V_O$ and $\text{Mn}^{2+}-V_O$ centers in the perovskite compounds are given. In the third column, \bar{b}_2 is the \bar{b}_2 value extrapolated from the MgO $\bar{b}_2(R)$ function for the specific dis-

TABLE III. Intrinsic parameters \bar{b}_2 for Fe^{3+} and fluorine as ligand in some fluorine perovskite compounds.

	$T - T_c$ (K)	R_0 (Å)	φ (degree)	$10^3 (c/d - 1)$	Ref. cryst. data	b_2^0 (10^{-4} cm^{-1})	Ref. EPR data	$\bar{b}_2(F_0)t_2$ (cm^{-1})	$\bar{b}_2(R_0)$ (cm^{-1}) assuming $t_2 = 8$
TiCaF_3	43	2.198	3.3(2)	3.3(9)	42	50.4(10)	39	-0.76(23)	-0.095(28)
RbCdF_3	11	2.198	2.0(2)	1.5(5)	42	20.6(10)	40	-0.67(26)	-0.084(32)
RbCaF_3	40	2.229	3.2(2)	3.1(6)	43	37.3(10)	41	-0.61(14)	-0.076(17)

tance d displayed in the fifth column. If we compare the data in Table IV, we note that the Fe^{3+} - V_{O} and Mn^{2+} - V_{O} centers in the perovskite structure have a $b_2^0/\bar{b}_2(d)$ value of about -2 near $d = 2\text{Å}$.

To explain these $b_2^0/\bar{b}_2(d)$ values, we use the following model: (i) We first assume that the five oxygens are in the same positions as in the cubic phase. (ii) The Fe^{3+} ion can move in the direction of the C_{4v} axial symmetry axis. (iii) We assume that the power-law exponent for \bar{b}_2 is $t_2 = 8$.

From these assumptions, we calculate, in Fig. 1, curve a. In this figure, $b_2^0/\bar{b}_2(d)$ as a function of the movement of the Fe^{3+} or Mn^{2+} from the cubic site is shown. This movement is given in units of the undistorted distance d of the paramagnetic ion to the nearest ligand. From this figure, some characteristics can be obtained. If $\Delta = 0$, i.e., the paramagnetic ion is at the same place as in the cubic center, we get $b_2^0/\bar{b}_2 = -1$, a result expected for a missing ligand from Eq. (1). Negative Δ 's correspond to a motion of the paramagnetic ion in the direction opposite to the vacancy. Then we still get negative values of b_2^0/\bar{b}_2 down to $\Delta = -0.08$, but less negative than at $\Delta = 0$. For $\Delta < -0.08$, the sign of b_2^0/\bar{b}_2 changes. If Δ is positive, the paramagnetic ion moves towards the vacancy and more negative values than -1 are obtained. The very broad minimum in this model is at -1.4 . To obtain more negative values it is necessary to introduce a contraction of the four planar oxygens perpendicular to the $M-V_{\text{O}}$ axis. In Fig. 1, curves for contractions of 1%-5% of the undistorted distance d are shown labeled as C_1, C_2, \dots, C_5 . With such a contraction, it is possible to explain values $b_2^0/\bar{b}_2(d)$ of about -2 . The broad minimum appears in all cases. For a 4% contraction ($C = 0.04$) a minimum of -2.1 at $\Delta_{\text{min}} = 0.09$ is reached. Here $\Delta = 0.09$ means a displacement of 0.18Å towards the vacancy for $d = \frac{1}{2}a = 2 \text{Å}$. For this curve, values of -2 to -2.1 are available in the range from $\Delta = 0.04$ (0.08Å) to $\Delta = 0.15$ (0.3Å). From this fact it is understandable that in different compounds where the Fe^{3+} and Mn^{2+} movements differ, about the same values of $b_2^0/\bar{b}_2(d)$ are reached. The contraction of 4% agrees well with the reduction of the ionic radius of the Fe^{3+} ion by the change of coordination number from 6 to 5 as listed by Megaw.⁴⁸

From this consideration, we expect that the paramagnetic ion is displaced towards the vacancy ($\Delta > 0$). This result has not been discussed so far in the literature. In the paper by von Waldkirch, Müller, and Berlinger⁵ on the Fe^{3+} vacancy center, it was assumed that Δ was negative. A negative Δ was assumed earlier by Zítková, Žďánský, and Šroubek⁴⁹ for the Ti^{3+} - V_{O} center. These authors

TABLE IV. $M-V_O$ pair centers in oxide perovskite compounds.

Center	b_2^0 (cm $^{-1}$)	$\bar{b}_2(d)$ (cm $^{-1}$) extr. MgO	$b_2^0/\bar{b}_2(d)$	Ref. point d (Å)	Ref. for EPR data
Fe $^{3+}$ - V_O in SrTiO $_3$	1.350(15)	-0.74(11)	-1.82(27)	1.952	5
Fe $^{3+}$ - V_O in KTaO $_3$	1.44(1)	-0.63(8)	-2.29(30)	1.994	45
Fe $^{3+}$ - V_O in PbTiO $_3$	1.187(2)	-0.45(4)	-2.64(22)	2.076	46
Mn $^{2+}$ - V_O in SrTiO $_3$	0.5440(5)	-0.26(3)	-2.09(24)	1.952	7
					47

had proposed an intrinsic vacancy model Ti $^{3+}$ - V_O for Ti $^{3+}$ in BaTiO $_3$ in which the Ti $^{3+}$ ion was displaced about 0.4 Å in the opposite direction to the vacancy ($\Delta = -0.2$). This displacement would give a value of $b_2^0/\bar{b}_2(d) > 0$ for Fe $^{3+}$, which is in contradiction to the positive sign of b_2^0 and the negative values of \bar{b}_2 found here. The present consideration confirms a criticism of the work of Zítková *et al.*⁴⁹ by Müller, Berlinger, and Rubins,⁵⁰ who pointed out that the Ti $^{3+}$ EPR data result from an extrinsic Ti $^{3+}$ center and not from an intrinsic Ti $^{3+}$ - V_O -Ti $^{4+}$ center.

The tilt angle of the octahedra in the tetragonal phase of SrTiO $_3$ is an important piece of evidence that $\Delta > 0$ is correct. In the paper on the EPR analysis of the Fe $^{3+}$ - V_O pair center in the tetragonal phase of SrTiO $_3$, the tilt $\bar{\varphi}$ of the Fe $^{3+}$ - V_O center is lower than that of the normal octahedral rotation angle φ ($\varphi = 1.6 \bar{\varphi}$).⁵ In a simple model (see Fig. 2), we assume that the displacement of oxygen numbered 4 is the same in both the distorted and undistorted cases, and the turning point is the Fe $^{3+}$ ion. With these assumptions we get

$$\tan \varphi / \tan \bar{\varphi} = 1 + \Delta.$$

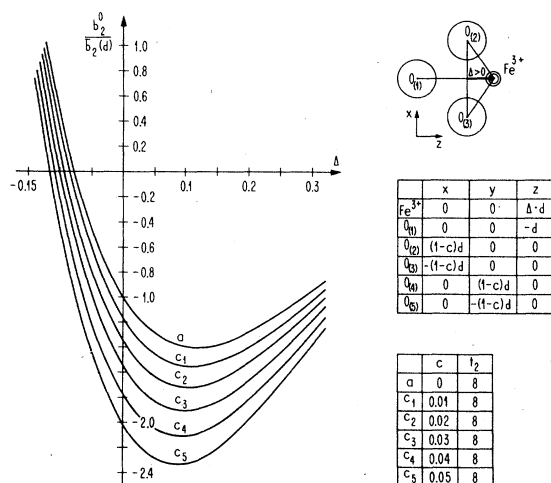


FIG. 1. Local environment, coordination of the ions, and the prediction of $b_2^0/\bar{b}_2(d)$ for an $M-V_O$ center with different contractions of the four planar oxygen ions.

If $\Delta < 0$ we get $\varphi < \bar{\varphi}$, and with $\Delta > 0$ we obtain $\varphi > \bar{\varphi}$. To account for the experimental fact $\varphi > \bar{\varphi}$, we have to use $\Delta > 0$. In this simple model, the value itself is not obtainable. With $\Delta = 0.1$ (see Fig. 1) one would get $\varphi = 1.1 \bar{\varphi}$, which is too low compared with the measured values. Schirmer, Berlinger, and Müller⁶ found an identical distortion angle $\bar{\varphi}$ for the Fe $^{4+}$ - V_O as for the Fe $^{3+}$ - V_O pair center. Therefore, the geometry must be the same. This shows that Coulomb interaction does not play an important role for the center as in one case where the iron is nominally tetravalent and in the other trivalent. Thus it follows that the core repulsion is dominant, forcing the metal ion towards the vacancy V_O , i.e., $\Delta > 0$.

From our consideration, the Fe $^{3+}$ - V_O and the Mn $^{2+}$ - V_O centers in oxygen perovskite structure compounds can be characterized as follows. (i) The centers have dominantly axial C_{4v} symmetry. (ii) The sign of b_2^0 is positive, i.e., the $E(m = \pm \frac{1}{2})$ energy level is lowest in energy. (iii) The ratio of b_2^0 and $\bar{b}_2(d)$ of Eq. (3) is about -2. (iv) The Fe $^{3+}$ and Mn $^{2+}$ ions are displaced by about 0.2 Å towards the vacancy. The planar ion distances are contracted by about 4%. Together this gives a deformation angle of about 6° from the Fe $^{3+}$ to the basal four oxygens.

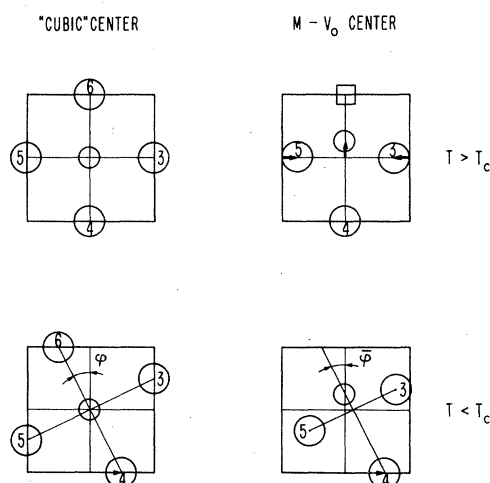


FIG. 2. Tilt angle for the "cubic" and $M-V_O$ pair center in SrTiO $_3$.

V. DISCUSSION OF SOME AXIAL CENTERS

In this section, we use the superposition model to assign centers to local configurations and to distinguish between different models.

A. Axial MgO and SrO centers

In the NaCl-type compounds, axial centers in MgO:Fe³⁺ (Ref. 12) and SrO:Mn²⁺ (Ref. 13) were reported by Henderson *et al.*¹² and Rubio *et al.*,¹³ respectively. The data of these centers are given in Table V. They are characterized by the positive sign of b_2^0 and the ratio of $b_2^0/\bar{b}_2(d)$ close to -1.2 for both ions. In the case of MgO, Henderson *et al.*¹² assigned this center as a next-nearest-neighbor cation vacancy center V_{Mg} . For SrO:Mn²⁺, Rubio *et al.* did not discuss where the axiality of this center originated.¹³ A comparison of the ratio $b_2^0/\bar{b}_2(d) = -1.2$ with the calculation for an $M-V_O$ pair center displayed in Fig. 1, curve a, shows that the ratio can be explained within this model. However, it differs from that in the perovskites of -2 . On the other hand, the packing in the second shell is different between NaCl and ABX_3 perovskite compounds. In the following, we discuss why we believe that the axial centers could be $M-V_O$ pair centers and that a V_{Mg} assignment is not correct.

The arrangement of the ions for a V_{Mg} center is shown in Fig. 3. We assume that the Fe³⁺ ion and the five oxygens are on their cubic sites, respectively. The sixth oxygen ion sits and moves on the axis of the paramagnetic ion and Mg vacancy. The motion is described by the distance of the Fe³⁺ ion to this oxygen with the use of a parameter c measured in units of the undistorted oxygen distance d . This parameter c is zero for the oxygen at its intrinsic site, greater than zero for oxygen movements towards the Fe³⁺ ion, and less than zero for movements towards the Mg vacancy. The superposition model predicts $b_2^0/\bar{b}_2(d) = (1-c)^{-2} - 1$. In Fig. 3, $b_2^0/\bar{b}_2(d)$ vs the parameter c is shown for $t_2 = 8$. For $c > 0$ the ratio is always positive, which is in contradiction to the measured values. For $c < 0$, i.e., the oxygen moving towards the vacancy, we get the right sign of $b_2^0/\bar{b}_2(d)$, but the values are too low [for $c = 22\%$, $b_2^0/\bar{b}_2(d) = -0.8$ or $c = 33\%$, $b_2^0/\bar{b}_2(d) = -0.9$]. If we assume that the Coulomb inter-

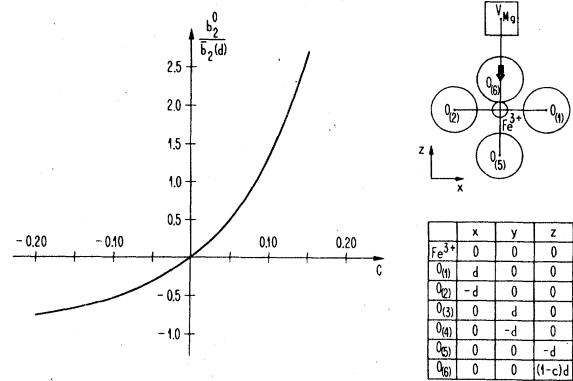


FIG. 3. Local environment, coordinates of the ions, and the prediction of $b_2^0/\bar{b}_2(d)$ for an Mg vacancy center V_{Mg} .

action is the important one in MgO, then we expect that the oxygen ion is near the Fe³⁺ ion repelled by the charge of the vacancy ($c > 0$).

We now show that the simple model for the cation vacancy centers predicts correctly the positive sign of the parameter c in the fluoride perovskites. The V_{Zn} center in $KZnF_3$ and the V_{Cd} centers in $KCdF_3$, $RbCdF_3$, and $CsCdF_3$, all doped with Fe³⁺, have been observed.⁵¹ The sign of b_2^0 is always negative, resulting in a positive ratio of $b_2^0/\bar{b}_2^F(d)$ since \bar{b}_2^F is negative. In Table VI the b_2^0 values for the different compounds are displayed. As a rough estimate, and assuming that the intrinsic parameter for the fluorine compounds is $\bar{b}_2^F(d) = -0.09(3)$ cm⁻¹ (Sec. III B.), we get the entries of the last column. For the V_{Cd} centers, we obtain $b_2^0/\bar{b}_2(d)$ of about $+0.5$, yielding a contraction $c \approx +5\%$, and for the V_{Zn} center we get $c \approx +7\%$.

Another argument against the assignment of a V_{Mg} center in MgO:Fe³⁺ is based on the correlation of the b_2^0 parameters between Fe³⁺ and Cr³⁺. From oxide crystals, Müller⁵² found $b_2^0(Fe^{3+}) = \alpha_1 b_2^0(Cr^{3+})$ with $\alpha_1 = 0.87$. Henderson and Hall⁴ reported in MgO a Cr³⁺ center which they assigned as a Cr³⁺-O²⁻- V_{Mg} center with $b_2^0 = 819.5 \times 10^{-4}$ cm⁻¹, which was previously found by Wertz and Auzins.² If we assume that the above-mentioned Fe³⁺ center is an Fe³⁺-O²⁻- V_{Mg} center, then we would get $b_2^0(Fe^{3+})/b_2^0(Cr^{3+}) = 5.7$. This ratio is much too large compared with 0.87. Therefore, the assignment of

TABLE V. Axial centers in NaCl-type compounds.

	b_2^0 (cm ⁻¹)	\bar{b}_2 (cm ⁻¹) extr. MgO	$b_2^0/\bar{b}_2(d)$	d (Å)	Ref. EPR data
MgO:Fe ³⁺	+0.470	-0.412(25)	-1.14(8)	2.101	12
SrO:Mn ²⁺	+0.045 44(8)	-0.035(12)	-1.30(40)	2.572	13

TABLE VI. V_{Zn} and V_{Cd} centers in some fluorine perovskite compounds doped with Fe^{3+} at 300 K. ^a

	d (Å)	b_2^0 (10^{-4} cm $^{-1}$)	\bar{b}_2^F (cm $^{-1}$)	b_2^0/\bar{b}_2^F
KZnF ₃	2.027	-759.0(5)	-0.09(3)	+0.84(28)
KCdF ₃	2.167	-400.0(100)	-0.09(3)	+0.44(15)
RbCdF ₃	2.197	-422.2(5)	-0.09(3)	+0.47(18)
CsCdF ₃	2.23	-548.8(5)	-0.09(3)	+0.61(20)

^a EPR data from Ref. 51.

both centers to a V_{Mg} center is not consistent. The same conclusion was recently arrived at by de Biasi and Caldas.⁵³ A $Cr^{3+}-V_O$ center is not probable as Meierling⁵⁴ has shown, since Cr^{3+} is always found in sixfold coordination. Therefore, the axial Cr^{3+} center in MgO should be a $Cr^{3+}-O^{2-}-V_{Mg}$ center. Since the b_2^0 relation for Fe^{3+} and Cr^{3+} ions is not fulfilled, the only option we have is to assume an $Fe^{3+}-V_O$ pair center. Such a center can occur, as demonstrated in SrTiO₃.

We can also discard a possible off-center position of the Fe^{3+} and Mn^{2+} ions because cubic spectra in MgO: Fe^{3+} and SrO: Mn^{2+} were reported.^{13,55} The superposition model also predicts for such a center $b_2^0/\bar{b}_2^F(d) > 0$ as shown in Fig. 4, which is at variance with the measured signs.

From these considerations, we expect that the axial centers in MgO: Fe^{3+} and SrO: Mn^{2+} are $Fe^{3+}-V_O$ and $Mn^{2+}-V_O$ pair centers, respectively. The $Fe^{3+}-V_O$ center would be three and the $Mn^{2+}-V_O$ center two times positively charged with respect to the MgO and SrO lattices, respectively. This seems unlikely. However, in SrTiO₃, the $Fe^{4+}-V_O$ center with two positive charges with respect to the lattice has been shown to exist.⁶

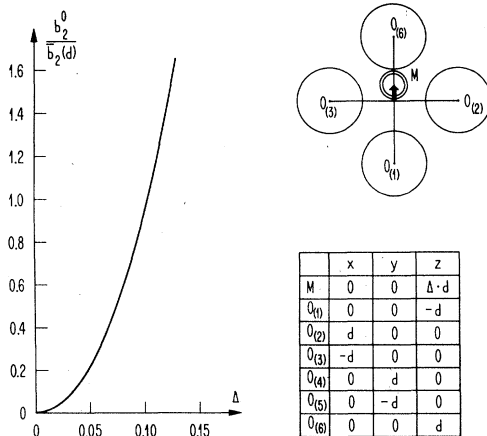


FIG. 4. Local environment, coordinates of the ions, and the prediction of $b_2^0/\bar{b}_2^F(d)$ for an off-center position of Mn^{2+} and Fe^{3+} in an oxygen octahedra.

B. Strong axial Fe^{3+} centers in some fluorine perovskite compounds

In recent years, three strongly axial Fe^{3+} centers in KMgF₃,¹⁴ KZnF₃,¹⁵ and RbCdF₃,¹⁶ were reported. In Table VII, the values of these centers are presented. The greatest controversy about the data is the *sign of b_2^0* . In KMgF₃ it was reported to be positive and in KZnF₃, negative, but the magnitudes are almost the same. The ratio $|b_2^0/\bar{b}_2^F|$ is about 3 ± 1 , if we assume a constant intrinsic parameter \bar{b}_2^F .

ENDOR data in KMgF₃ of Stjern, DuVarney, and Unruh¹⁴ showed that one of the six fluorine ions is missing or replaced by a charge-compensating impurity such as O^{2-} and that the Fe^{3+} ion is moving towards the defect. In the discussion, they concluded that the center is probably an FeOF₅ cluster, because they did not expect the Fe^{3+} ion to move towards the defect without a two-fold negatively charged impurity. In KZnF₃, Buzaré and Fayet¹⁵ concluded that b_2^0 has to be negative to get a positive cubic a value. They called this center an FeOF₅ cluster.

Since the g value, the superhyperfine parameters, and the magnitude of the b_2^0 values are similar, the origin of these centers should be the same. However, this would require the same sign of b_2^0 for all three compounds. We use the superposition model to distinguish between the $Fe^{3+}-V_F$ pair and the FeOF₅ cluster centers.

For the FeOF₅ cluster we first take a simple model without motion of the Fe^{3+} against the defect. Thus, assuming the Fe^{3+} ion is on the cubic position, and one F⁻ site is occupied by an O^{2-} ion, one obtains

$$b_2^0(FeOF_5) = \bar{b}_2^O(d) - \bar{b}_2^F(d).$$

Since $|\bar{b}_2^O|$ is about three times larger than $|\bar{b}_2^F|$ and both are negative, $b_2^0(FeOF_5)$ has a negative sign. In Table VII (last column) the $b_2^0(FeOF_5)$ values for the three compounds are displayed. Here we assume a constant value for the fluorine intrinsic parameter because the distance dependence is not well known (Sec. III B). In all compounds, a negative sign is found. Introducing a movement of the Fe^{3+} ion, the values become more negative because the distance between the Fe^{3+} and oxygen ions becomes smaller, resulting in an increase of the \bar{b}_2^O parameter. In Fig. 5, as an example, b_2^0 vs the distance Δ of the Fe^{3+} ion from the cubic position for KZnF₃ is plotted. From the ENDOR data it is known that Δ (the normalized distance from the cubic position in units of the undistorted distance) is greater than zero. b_2^0 is always negative and $|b_2^0|$ is larger than the absolute value 0.46 cm $^{-1}$ at $\Delta = 0$. To get lower absolute values,

TABLE VII. Strong axial Fe^{3+} centers in some fluorine perovskite compounds.

	$ b_2^0 $ (cm^{-1})	Sign of b_2^0	Ref. for EPR data	d (\AA)	$\bar{b}_2^0(d)$ (cm^{-1})	$\bar{b}_2^F(d)$ (cm^{-1})	$ b_2^0/\bar{b}_2^F $	b_2^0 (FeOF_5) (cm^{-1})
KMgF_3	0.352(5)	+	14	1.986	-0.65(8)	-0.09(3)	3.9 ± 1.3	-0.56(11)
KZnF_3	0.301(1)	-	15	2.027	-0.55(7)	-0.09(3)	3.3 ± 1.1	-0.46(9)
RbCdF_3	0.210	?	16	2.199	-0.29(3)	-0.09(3)	2.8 ± 0.8	-0.20(6)

it is necessary to introduce a contraction of the four fluorine ions in the plane perpendicular to the defect. An example is shown in Fig. 5 (curve c). In the case of KZnF_3 it would be possible to explain $b_2^0 = -0.3 \text{ cm}^{-1}$ for a contraction of 4% (0.08 \AA) and a movement of Fe^{3+} towards the defect by $\Delta = 0.02$ (0.04 \AA), and furthermore, taking the lowest value of $|\bar{b}_2^0|$ and the highest value of $|\bar{b}_2^F|$. Therefore, it is, in principle, possible to explain the values with the FeOF_5 cluster model. However, it is not obvious why the fluorine ions should move towards the Fe^{3+} ion. A negative sign of the b_2^0 value which is necessary for an FeOF_5 cluster is reported in KZnF_3 , but not in KMgF_3 .

The other possible explanation for the measured b_2^0 values is a fluorine vacancy (V_F). The rough estimation of $|b_2^0/\bar{b}_2^F|$ of about 3 ± 1 is somewhat larger than in the oxygen perovskite compounds, but larger contractions of the four planar ligands could yield such values. Since the fluorine and the oxygen intrinsic parameters \bar{b}_2 have the same sign, we get, using the calculation of Sec. IV, a positive sign of b_2^0 . This would agree in the KMgF_3 compound, but not with the sign reported

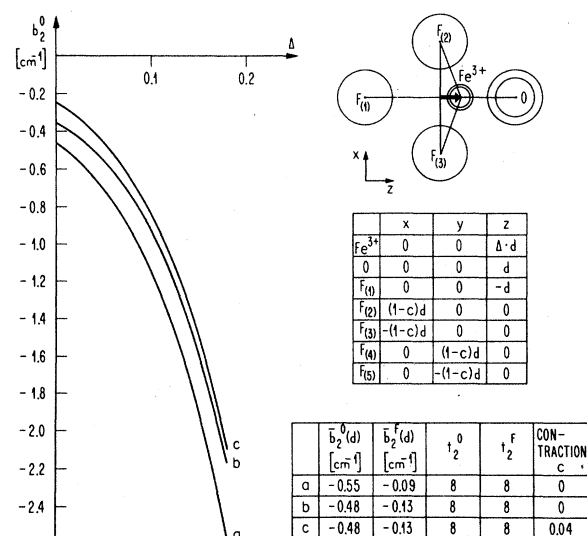


FIG. 5. Microscopic environment, coordinates of the ions, and model parameters for the calculation of b_2^0 for an FeOF_5 cluster center in KZnF_3 .

for KZnF_3 . The main distinction between the $\text{Fe}^{3+}-V_F$ pair and the FeOF_5 cluster centers is the different sign of b_2^0 . An $\text{Fe}^{3+}-V_F$ center yields a positive and the FeOF_5 cluster center, a negative sign of b_2^0 . Thus measurements of the signs of b_2^0 in the three compounds at low temperatures should answer this question.

A hint that the center is an FeOF_5 cluster comes from comparison with the Cr^{3+} center in KMgF_3 . From independent measurements, Patel *et al.*⁵⁶ and Abdulsabirov *et al.*⁵⁷ found a tetragonal center with $|b_2^0| = 0.217 \text{ cm}^{-1}$. The authors of Ref. 57 reported that the center appears after sample heat treatment in oxygen for 10 h at 850°C . Therefore, they assigned this center to a CrOF_5 cluster. Using Meierling's⁵⁴ argument that Cr^{3+} is normally found with a six nearest-neighbor coordination and avoids a five nearest-neighbor coordination, the $\text{Cr}^{3+}-V_F$ center is not acceptable. Furthermore, Müller⁵² showed that the ratio of the coefficients $b_2^0(\text{Fe}^{3+})/b_2^0(\text{Cr}^{3+})$ for oxides is 0.87. In Table VIII, some data for this ratio for fluorine ligands are shown, using the data of the V_{Cd} , V_{Zn} centers in the fluorine perovskite compounds of Rousseau *et al.*⁵¹ From this table, we conclude that about the same ratio for Fe^{3+} and Cr^{3+} b_2^0 values is valid for fluorine and oxygen ligands. Using the Fe^{3+} data of Table VII for KMgF_3 with the Cr^{3+} value discussed above, we get $|b_2^0(\text{Fe}^{3+})/b_2^0(\text{Cr}^{3+})| = 1.62$. This is in the approximate range of the ratios obtained above for fluoride and oxide compounds. Therefore, the Fe^{3+} and Cr^{3+} centers in KMgF_3 should have the same local surrounding. Thus, the Fe^{3+} center in KMgF_3 may also be an FeOF_5 cluster center. The sign of b_2^0 should therefore be negative.

TABLE VIII. Correlation of Fe^{3+} and Cr^{3+} axial spin-Hamiltonian parameters. EPR data from Ref. 51.

	b_2^0 (Fe^{3+})	b_2^0 (Cr^{3+})	b_2^0 (Fe^{3+})/ b_2^0 (Cr^{3+})
KZnF_3	-759.0(5)	-540.9(5)	1.40
KCdF_3	-400.0(100)	-545.0(70)	0.73
RbCdF_3	-422.2(5)	-569.0(5)	0.74
CsCdF_3	-548.8(5)	-628.6(5)	0.87

APPENDIX A: DETERMINATION OF THE SITE OF Mn^{2+}
IN $BaTiO_3$

Ikushima¹⁷ reported EPR results on Mn^{2+} in tetragonal $BaTiO_3$ single crystals. He found $b_2^0 = (215 \pm 2) \times 10^{-4} \text{ cm}^{-1}$ and assigned the Mn^{2+} center to a Ba^{2+} site. Three arguments lead us to the conclusion that the Mn^{2+} is on a Ti^{4+} site.

A. Cubic parameter a

The argument is based on two facts. (i) We use the superposition model for the $n=4$ parameters, and use the cubic parameter a for the Ti^{4+} and Ba^{2+} sites. Both sites were assumed to be occupied by Fe^{3+} or Mn^{2+} ions, respectively. Then we get

$$a(\text{Ti}^{4+} \text{ site}) = 7\bar{b}_4(d),$$

$$a(\text{Ba}^{2+} \text{ site}) = -\frac{7}{2}\bar{b}_4(d\sqrt{2}),$$

with

$$\bar{b}_4(d) = \bar{b}_4(d\sqrt{2})2^{t_4/2}.$$

We obtain

$$\frac{a(\text{Ti}^{4+} \text{ site})}{a(\text{Ba}^{2+} \text{ site})} = -2^{t_4/2+1}.$$

From different compounds, Müller⁵⁸ found for Fe^{3+} a power-law exponent of $t_4 = 6-7$ valid in the range $d = 1.9-2.4 \text{ \AA}$. If we assume that the $t_4 = 6$ power law is valid until about 2.8 \AA , we get a ratio of the a values of -16 . Assuming $t_4 = 5$ we obtain -11.2 . In $KTaO_3$ doped with Fe^{3+} , Hannon⁵⁹ reported a values for the dodecahedral and octahedral sites. For the ratio of a values at room temperature, one gets $9.6(5)$ and, at 4.2 K , $8.8(3)$. An appreciable inward relaxation of the oxygens probably occurs for the dodecahedral site. From this consideration, we can assume that the absolute ratio of the a values for Fe^{3+} , between the two sites, is of the order 10.

(ii) From the a values in MgO the ratio for Fe^{3+} and Mn^{2+} on an octahedral oxygen site is⁵⁴

$$a(Fe^{3+}, MgO)/a(Mn^{2+}, MgO) = 11.0.$$

We can now assume that this is also the correct ratio between the Fe^{3+} and Mn^{2+} cubic splittings for $BaTiO_3$ at an octahedral site. Assuming that t_4 for Fe^{3+} and Mn^{2+} are similar, then this ratio should also be valid for the dodecahedral site. This is the same argument as used for b_2^0 in Sec. II, Eq. (4).

In the cubic phase of $BaTiO_3$, Sakudo²⁶ found for Fe^{3+} at the Ti^{4+} site an a value with $a = (102 \pm 10) \times 10^{-4} \text{ cm}^{-1}$. From this value, one computes using (ii), for Mn^{2+} at the Ti^{4+} site,

$$a_{\text{expected}}(Mn^{2+} \text{ on } Ti^{4+}, BaTiO_3) \approx 9 \times 10^{-4} \text{ cm}^{-1}.$$

On the other hand, starting again from Fe^{3+} on the Ti^{4+} site, for Fe^{3+} on the Ba^{2+} site using (i) we get

$$a_{\text{expected}}(Fe^{3+} \text{ on } Ba^{2+}, BaTiO_3) \approx 10 \times 10^{-4} \text{ cm}^{-1}.$$

Using (ii) again, we now arrive at Mn^{2+} at the Ba^{2+} site with

$$a_{\text{expected}}(Mn^{2+} \text{ on } Ba^{2+}, BaTiO_3) \approx 0.9 \times 10^{-4} \text{ cm}^{-1}.$$

Ikushima¹⁷ found for Mn^{2+} in $BaTiO_3$ in the cubic phase $a = (12.11 \pm 0.94) \times 10^{-4} \text{ cm}^{-1}$ and, in the tetragonal phase, $a = (16.76 \pm 0.94) \times 10^{-4} \text{ cm}^{-1}$. Both values are of the order expected for Mn^{2+} on the Ti^{4+} site and more than an order of magnitude larger than the value expected for the Ba^{2+} site.

B. Hyperfine coupling constant A

Ikushima¹⁷ measured in the cubic phase $A = (-79.3 \pm 0.4) \times 10^{-4} \text{ cm}^{-1}$ and in the tetragonal phase

$$\bar{A} = \frac{1}{3}(A_z + 2A_x) = (-80.7 \pm 0.8) \times 10^{-4} \text{ cm}^{-1}.$$

These values are near the value of Mn^{2+} in $SrTiO_3$, $A = (-82.6 \pm 0.1) \times 10^{-4} \text{ cm}^{-1}$,⁴⁷ from which it is known that Mn^{2+} is on the Ti^{4+} site. This value is also near the value of Mn^{2+} in MgO , $A = (-81.0 \pm 0.2) \times 10^{-4} \text{ cm}^{-1}$, where Mn^{2+} has an octahedral surrounding.⁵⁵ On the other hand, using the curve of the hyperfine constant A versus the covalency parameter c/n in the work of Šimánek and Müller,³⁸ one expects for a coordination number $n=6$, $A \approx -86 \times 10^{-4} \text{ cm}^{-1}$, and for $n=12$, $A \approx -96 \times 10^{-4} \text{ cm}^{-1}$, taking $c \approx 0.5$ for the Mn-O covalency parameter, and using Eq. (2) of Ref. 38 and the electronegativities of Ref. 37. Therefore, we assign the Mn^{2+} to a Ti^{4+} site. This argument is similar to the one that led to the reassignment of the Mn^{2+} to a Zr^{4+} site in $CaZrO_3$.⁴⁷

C. Spin-Hamiltonian parameter b_2^0

The basis of the argument is the assumption that the ratio of b_2^0 values for Fe^{3+} and Mn^{2+} ions on the same site should be in the range of the ratio of the intrinsic parameters, as shown in Sec. II, Eq. (4). A comparison of the b_2^0 values of Fe^{3+} and Mn^{2+} in the tetragonal phase of $BaTiO_3$ gives

$$\begin{aligned} v &= b_2^0(Fe^{3+}, BaTiO_3)/b_2^0(Mn^{2+}, BaTiO_3) \\ &= 4.3(1). \end{aligned}$$

This value is in the range

$$w = \bar{b}_2(Fe^{3+}, MgO)/\bar{b}_2(Mn^{2+}, MgO) = 2.71(25).$$

From the b_2^0 value used by Sakudo²⁶ for Fe^{3+} in

tetragonal BaTiO₃, it is clear that the Fe³⁺ ion is on the Ti⁴⁺ site; therefore we conclude that the b_2^0 value of Mn²⁺ results from the same site.

Ikushima and Hayakawa⁶⁰ also reported an axial Mn²⁺ spectrum that they attributed to an Mn²⁺ ion being on a Ti⁴⁺ site. If we used the value of this center $b_2^0 = (65 \pm 5) \times 10^{-4} \text{ cm}^{-1}$, we would get $v = 14.3 \pm 1.3$ with the same b_2^0 value for Fe³⁺ as above. This ratio v is too large compared with $w = 2.7$. Thus the spectrum with $b_2^0 = 65 \times 10^{-4} \text{ cm}^{-1}$ does not come from an Mn²⁺ ion on a Ti⁴⁺ site.

From the three arguments about a , A , and b_2^0 , we conclude that the Mn²⁺ center with $b_2^0 = 215 \times 10^{-4} \text{ cm}^{-1}$ belongs to an Mn²⁺ center that is on a Ti⁴⁺, and not a Ba²⁺, site.

APPENDIX B: AXIAL CENTER OF Mn²⁺ IN KTaO₃

In the list of $M-V_O$ pair centers in perovskite compounds (Table IV), the Mn²⁺ center in KTaO₃ from Hannon,¹⁸ which he attributed to an Mn²⁺- V_O pair center, was not included. In the work of Serway, Berlinger, Müller, and Collins,⁴⁷ it was shown that there exist arguments against this assignment based on the spin-Hamiltonian parameter b_2^0 and the hyperfine-splitting parameter A . They proposed that Mn²⁺ should be on the K⁺ site with either a K vacancy next to it or an Mn²⁺ sitting off center. From the value of A , they estimated that the Mn²⁺ should have about nine oxygens surrounding it. The superposition model also shows that the interpretation of this axial center with $b_2^0 = +0.147 \text{ cm}^{-1}$ requires a different configuration from the $M-V_O$ centers of Table IV. This is based on the b_2^0/\bar{b}_2 ($d = \frac{1}{2}a$) value. For the Ta⁵⁺ site, we get for the intrinsic parameter, at the undistorted distance to the oxygens, \bar{b}_2 ($d = \frac{1}{2}a$) = $-0.23(3) \text{ cm}^{-1}$ and, therefore, b_2^0/\bar{b}_2 ($d = \frac{1}{2}a$) = $-0.65(8)$. This value is very low compared to that of SrTiO₃:Mn²⁺ with $-2.09(24)$; therefore, we omitted this Mn²⁺ center in Table IV.

According to the suggestion of Serway *et al.*⁴⁷ that Mn²⁺ should be on the K site, the distance to the 12 oxygens is $d = a/\sqrt{2}$. Using this distance as a reference point for this site, we get $b_2^0/\bar{b}_2(a/\sqrt{2}) = -7.4 \pm 2.4$. In Fig. 6, the K site surroundings are shown. We now assume that Mn²⁺ is off center and all the oxygens remain in their

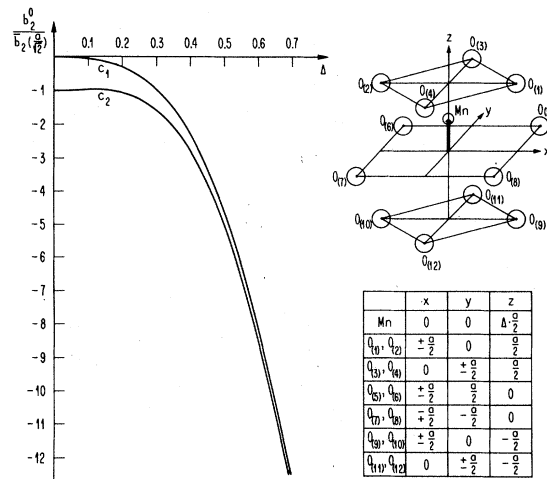


FIG. 6. Local environment, ion positions, and the calculation of $b_2^0/\bar{b}_2(a/\sqrt{2})$ for an off-center Mn²⁺ in an A site of the perovskite compound ABO₃.

cubic positions. The off-center Mn²⁺ is characterized by the deviation Δ from the ideal K site in units of $\frac{1}{2}a$, i.e., the separation between the oxygen planes. In Fig. 6 (curve c_1), $b_2^0/\bar{b}_2(a/\sqrt{2})$ vs Δ is shown for the power-law exponent $t_2 = 7$. It can be seen that $b_2^0/\bar{b}_2(a/\sqrt{2}) = -7.4$ is obtainable if we assume that the Mn²⁺ ion is located at $\Delta = 0.58$, or, including the errors of $b_2^0/\bar{b}_2(a/\sqrt{2}), \Delta = 0.50-0.64$. That means that if the Mn²⁺ is somewhat above the middle of the two upper oxygen planes, the sign and amount of b_2^0 for Mn²⁺ in KTaO₃ is explicable. In curve c_2 of Fig. 6, we calculated the same quantities as in curve c_1 , but with oxygens one to eight only. It is clear that both curves are near each other for $\Delta > 0.4$. From this we can conclude that oxygens 9-12 bring only small additions to the $b_2^0/\bar{b}_2(a/\sqrt{2})$ ratio.

Our calculation shows that a very strong off-center position is necessary to explain the measured value. Such an off-center position is not obvious because Hannon⁵⁹ found a cubic Fe³⁺ center in KTaO₃ on the K⁺ site. Since the ionic radius of Fe³⁺ is less than that of Mn²⁺,⁴⁸ it would be astonishing were Mn²⁺ on an off-center position and Fe³⁺ not. Therefore, the center may be an Mn²⁺- V_K center.

*Present address: Institut für Angewandte Physik, Universität Bonn, D 5300 Bonn, Federal Republic of Germany.

¹E. S. Kirkpatrick, K. A. Müller, and R. S. Rubins, Phys. Rev. **135**, A86 (1964).

²J. E. Wertz and P. V. Auzins, Phys. Rev. **106**, 484

(1957).

³J. E. Wertz and P. V. Auzins, J. Phys. Chem. Solids **28**, 1557 (1967).

⁴B. Henderson and T. P. P. Hall, Proc. Phys. Soc. Lond. **90**, 511 (1967).

⁵Th. von Waldkirch, K. A. Müller, and W. Berlinger,

- Phys. Rev. B 5, 4324 (1972).
- ⁶O. F. Schirmer, W. Berlinger, and K. A. Müller, *Solid State Commun.* 16, 1289 (1975).
- ⁷R. A. Serway, W. Berlinger, and K. A. Müller, *Proceedings of the Eighteenth Ampere Congress*, edited by P. S. Allen, E. R. Andrew, and C. A. Bates (Nottingham University, Nottingham, 1974), p. 145.
- ⁸D. J. Newman, *Adv. Phys.* 20, 197 (1971).
- ⁹D. J. Newman and W. Urban, *J. Phys. C* 5, 3101 (1972).
- ¹⁰D. J. Newman and W. Urban, *Adv. Phys.* 24, 793 (1975).
- ¹¹D. J. Newman and E. Siegel, *J. Phys. C* 9, 4285 (1976).
- ¹²B. Henderson, J. E. Wertz, T. P. P. Hall, and R. D. Dowling, *J. Phys. C* 4, 107 (1971).
- ¹³J. Rubio, Y. Chen, and M. M. Abraham, *J. Phys. Chem. Solids* 38, 215 (1977).
- ¹⁴D. C. Stjern, R. C. DuVarney, and W. P. Unruh, *Phys. Rev. B* 10, 1044 (1974).
- ¹⁵J. Y. Buzaré and J. C. Fayet, *Phys. Status Solidi B* 74, 393 (1976).
- ¹⁶J. Y. Buzaré and J. C. Fayet, *Solid State Commun.* 21, 1097 (1977).
- ¹⁷H. Ikushima, *J. Phys. Soc. Jpn.* 21, 1866 (1966).
- ¹⁸D. M. Hannon, *Phys. Rev. B* 3, 2153 (1971).
- ¹⁹M. M. Curtis, D. J. Newman, and G. E. Stedman, *J. Chem. Phys.* 50, 1077 (1969).
- ²⁰Th. v. Waldkirch and K. A. Müller, *Helv. Phys. Acta* 46, 331 (1973).
- ²¹A. Okazaki and M. Kawaminami, *Ferroelectrics* 7, 91 (1974).
- ²²K. A. Müller, *Solid State Commun.* 9, 373 (1971).
- ²³B. Adefeld, *Z. Phys.* 222, 155 (1969).
- ²⁴K. A. Müller, *Helv. Phys. Acta* 31, 173 (1958).
- ²⁵J. Harada, T. Pedersen, and Z. Barnea, *Acta Crystallogr. A* 26, 336 (1970).
- ²⁶T. Sakudo, *J. Phys. Soc. Jpn.* 18, 1626 (1963).
- ²⁷G. Shirane, H. Danner, and R. Pepinsky, *Phys. Rev.* 105, 856 (1957).
- ²⁸A. W. Hewat, *J. Phys. C* 6, 2559 (1973).
- ²⁹E. Siegel, W. Urban, K. A. Müller, and E. Wiesendanger, *Phys. Lett. A* 53, 415 (1975).
- ³⁰G. Shirane, R. Pepinsky, and B. C. Frazer, *Acta Crystallogr.* 9, 131 (1956).
- ³¹R. G. Pontin, E. F. Slade, and D. J. E. Ingram, *J. Phys. C* 2, 1146 (1969).
- ³²H. Ikushima and S. Hayakawa, *J. Phys. Soc. Jpn.* 27, 414 (1969).
- ³³H. Arend, *Proceedings of the International Meeting on Ferroelectricity*, edited by V. Dvůrák, A. Fousková, and P. Glogar (Institute of Physics of the Czechoslovak Academy of Sciences, Prague, 1966), p. 231.
- ³⁴Vishwamittar and S. P. Puri, *J. Chem. Phys.* 61, 3720 (1974).
- ³⁵C. F. Hempstead and K. D. Bowers, *Phys. Rev.* 118, 131 (1960).
- ³⁶J. Bronstein and S. Maniv, *Phys. Rev.* 153, 303 (1967).
- ³⁷W. Gordy and W. J. O. Thomas, *J. Chem. Phys.* 24, 439 (1956).
- ³⁸E. Šimánek and K. A. Müller, *J. Phys. Chem. Solids* 31, 1027 (1970).
- ³⁹J. J. Rousseau, A. Leble, J. Y. Buzaré, J. C. Fayet, and M. Rousseau, *Ferroelectrics* 12, 201 (1976).
- ⁴⁰J. J. Rousseau and J. C. Fayet, *C. R. Acad. Sci., Ser. B* 281, 607 (1975).
- ⁴¹F. A. Modine, E. Sonder, W. P. Unruh, C. B. Finch, and R. D. Westbrook, *Phys. Rev. B* 10, 1623 (1974).
- ⁴²M. J. Rousseau, J. Y. Gesland, J. Julliard, J. Nouet, J. Zarembowitch, and A. Zarembowitch, *Phys. Rev. B* 12, 1579 (1975).
- ⁴³C. Ridou, M. Rousseau, J. Y. Gesland, J. Nouet, and A. Zarembowitch, *Ferroelectrics* 12, 199 (1976).
- ⁴⁴J. J. Krebs and R. K. Jeck, *Phys. Rev. B* 5, 3499 (1972).
- ⁴⁵G. Wessel and H. Goldick, *J. Appl. Phys.* 39, 4855 (1968).
- ⁴⁶O. Lewis and G. Wessel, *Phys. Rev. B* 13, 2742 (1976).
- ⁴⁷R. A. Serway, W. Berlinger, K. A. Müller, and R. W. Collins, *Phys. Rev. B* 16, 4761 (1977).
- ⁴⁸H. D. Megaw, *Crystal Structure: A Working Approach* (Saunders, Philadelphia, 1973).
- ⁴⁹J. Zítková, K. Žďánský, and Z. Sroubek, *Czech. J. Phys. B* 17, 636 (1967).
- ⁵⁰K. A. Müller, W. Berlinger, and R. S. Rubins, *Phys. Rev.* 186, 361 (1969).
- ⁵¹J. J. Rousseau, J. Y. Gesland, M. Binois, and J. C. Fayet, *C. R. Acad. Sci., Ser. B* 279, 103 (1974).
- ⁵²K. A. Müller, *Helv. Phys. Acta* 38, 358 (1965).
- ⁵³R. S. de Biasi and A. Caldas, *J. Phys. C* 10, 107 (1977).
- ⁵⁴H. D. Meierling, *Phys. Status Solidi B* 43, 191 (1971).
- ⁵⁵E. R. Feher, *Phys. Rev.* 136, A145 (1964).
- ⁵⁶J. L. Patel, J. J. Davies, B. C. Cavenett, H. Takeuchi, and K. Horai, *J. Phys. C* 9, 129 (1976).
- ⁵⁷R. Yu. Abdulsabirov, L. D. Livanova, and V. G. Stepanov, *Sov. Phys.-Solid State* 16, 1395 (1975).
- ⁵⁸K. A. Müller, *Ferroelectrics* 13, 381 (1976).
- ⁵⁹D. M. Hannon, *Phys. Rev.* 164, 366 (1967).
- ⁶⁰H. Ikushima and S. Hayakawa, *J. Phys. Soc. Jpn.* 19, 1986 (1964).